Brain Advance Access published January 3, 2013

doi:10.1093/brain/aws312 Brain 2013: Page 1 of 13 | 1

BRAIN
A JOURNAL OF NEUROLOGY

ISPD gene mutations are a common cause of congenital and limb-girdle muscular dystrophies

Sebahattin Cirak,[1] Aileen Reghan Foley,[1] Ralf Herrmann,[2] Tobias Willer,[3,4,5,6] Shu Yau,[7] Elizabeth Stevens,[1] Silvia Torelli,[1] Lina Brodd,[7] Alisa Kamynina,[1] Petr Vondracek,[8] Helen Roper,[9] Cheryl Longman,[10] Rudolf Korinthenberg,[11] Gianni Marrosu,[12] Peter Nürnberg,[13] UK10K Consortium,* Daniel E. Michele,[14] Vincent Plagnol,[15] Matt Hurles,[16] Steven A. Moore,[17] Caroline A. Sewry,[1,18] Kevin P. Campbell,[3,4,5,6] Thomas Voit[19] and Francesco Muntoni[1]

1 Dubowitz Neuromuscular Centre, UCL Institute of Child Health, University College London, WC1N 1EH London, UK
2 Zentrum fuer Kinderheilkunde, Paediatrie I, University Hospital Essen, 45145 Essen, Germany
3 Howard Hughes Medical Institute, University of Iowa Roy J and Lucille A Carver College of Medicine, Iowa City, Iowa, USA
4 Department of Molecular Physiology and Biophysics, University of Iowa Roy J. and Lucille A. Carver College of Medicine, Iowa City, IA 52242, USA
5 Department of Neurology, University of Iowa Roy J. and Lucille A. Carver College of Medicine, Iowa City, IA 52242, USA
6 Department of Internal Medicine, University of Iowa Roy J. and Lucille A. Carver College of Medicine, Iowa City, IA 52242, USA
7 DNA Laboratory, GSTS Pathology, Guy's Hospital, SE1 9RT, London, UK
8 University Hospital Brno, Department of Neurology, 62500 Brno, Brno, Czech Republic
9 Department Paediatrics, Birmingham Heartlands Hospital, B9 5SS Birmingham, UK
10 Department of Clinical Genetics, Yorkhill Hospital, G3 8SJ Glasgow, UK
11 Division of Neuropaediatrics and Muscular Disorders, Department of Paediatrics and Adolescent Medicine, University Hospital, Albert-Ludwigs University, 79106, Freiburg im Breisgau, Germany
12 Neuromuscular Unit, Multiple Sclerosis Centre, University of Cagliari, 09124, Cagliari, Italy
13 Cologne Centre for Genomics (CCG), Universität zu Köln, 50931, Cologne, Germany
14 Department of Molecular and Integrative Physiology, University of Michigan, Ann Arbor, MI 48109, USA
15 UCL Genetics Institute, University College London, WC1E 6BT, London, UK
16 Wellcome Trust Sanger Institute, Hinxton, CB10 1SA Cambridge, UK
17 Department of Pathology, University of Iowa Roy J. and Lucille A. Carver College of Medicine, Iowa City, IA 52242, USA
18 Wolfson Centre for Inherited Neuromuscular Disorders, RJAH Orthopaedic Hospital, SY10 7AG, Oswestry, UK
19 University Pierre et Marie Curie Paris VI, UM 76, INSERM U 974, CNRS UMR 7215, Institut de Myologie, Groupe Hospitalier Pitié-Salpêtrière, 75013 Paris, France

*The full list of members of the UK10K Consortium are available at www.uk10k.org/consortium.html.

Correspondence to: Francesco Muntoni,
Dubowitz Neuromuscular Centre,
UCL Institute of Child Health,
University College London,
30 Guilford Street, London WC1N 1EH, UK
E-mail: f.muntoni@ucl.ac.uk

Dystroglycanopathies are a clinically and genetically diverse group of recessively inherited conditions ranging from the most severe of the congenital muscular dystrophies, Walker–Warburg syndrome, to mild forms of adult-onset limb-girdle muscular dystrophy. Their hallmark is a reduction in the functional glycosylation of α-dystroglycan, which can be detected in muscle biopsies. An important part of this glycosylation is a unique *O*-mannosylation, essential for the interaction of α-dystroglycan with extracellular matrix proteins such as laminin-α2. Mutations in eight genes coding for proteins in the glycosylation pathway are responsible for ~50% of dystroglycanopathy cases. Despite multiple efforts using traditional positional cloning, the causative genes for unsolved dystroglycanopathy cases have escaped discovery for several years. In a recent collaborative study, we discovered that

Received April 18, 2012. Revised July 5, 2012. Accepted September 30, 2012

loss-of-function recessive mutations in a novel gene, called isoprenoid synthase domain containing (*ISPD*), are a relatively common cause of Walker–Warburg syndrome. In this article, we report the involvement of the *ISPD* gene in milder dystroglycanopathy phenotypes ranging from congenital muscular dystrophy to limb-girdle muscular dystrophy and identified allelic *ISPD* variants in nine cases belonging to seven families. In two ambulant cases, there was evidence of structural brain involvement, whereas in seven, the clinical manifestation was restricted to a dystrophic skeletal muscle phenotype. Although the function of *ISPD* in mammals is not yet known, mutations in this gene clearly lead to a reduction in the functional glycosylation of α-dystroglycan, which not only causes the severe Walker–Warburg syndrome but is also a common cause of the milder forms of dystroglycanopathy.

Keywords: congenital muscular dystrophy; limb-girdle muscular dystrophy; dystroglycan; laminin; isoprenoid synthase

Abbreviations: CDP-ME = 4-diphosphocytidyl-2-methyl-D-erythritol synthase; LGMD = limb-girdle muscular dystrophy

Introduction

Congenital muscular dystrophies and limb-girdle muscular dystrophies (LGMDs) are characterized by hypotonia, muscle weakness, variable appearance of contractures and dystrophic changes on skeletal muscle biopsy. Although the congenital muscular dystrophies present either congenitally or during the first 6 months of life, the LGMDs present in late childhood, adolescence or adulthood (Voit, 1998; Bonnemann and Finkel, 2002). A number of genetically distinct entities have been identified within the congenital muscular dystrophies and LGMDs that are classified according to clinical and pathological criteria. An important subgroup, collectively known as the 'dystroglycanopathies', is associated with a reduction in the functional glycosylation of α-dystroglycan (Muntoni and Voit, 2004). Dystroglycan is composed of two subunits, α and β, which are post-translationally cleaved to give rise to a transmembrane (β) and external membrane protein (α), which is heavily *O*-glycosylated (Stalnaker *et al*., 2011). An important part of this glycosylation is a unique *O*-mannosylation sugar moiety that is involved in the interaction of α-dystroglycan with extracellular matrix proteins, such as laminin, agrin, perlecan, neurexin and pikachurin (Kanagawa and Toda, 2006; Waite *et al*., 2012). Mutations in eight genes coding for putative or demonstrated glycosyltransferases or other proteins involved in the α-dystroglycan glycosylation pathway have been identified in the dystroglycanopathies: protein *O*-mannosyltransferase 1 (*POMT1*; OMIM 607423) (Beltran-Valero de Bernabe *et al*., 2002), protein *O*-mannosyltransferase 2 (*POMT2*; OMIM 607439) (van Reeuwijk *et al*., 2005), protein *O*-mannose β-1, 2-*N*-acetylglucosaminyltransferase (*POMGNT1*; OMIM 606822) (Yoshida *et al*., 2001), fukutin (*FKTN*; OMIM 607440) (Kobayashi *et al*., 1998), fukutin-related protein (*FKRP*; OMIM 606596) (Brockington *et al*., 2001a), like-acetylglucosaminyltransferase (*LARGE*; OMIM 603590) (Longman *et al*., 2003) and dolichyl-phosphate mannosyltransferase polypeptide 3 *(DPM3*; OMIM 605951) (Lefeber *et al*., 2009). Recently, a missense mutation in the *DPM3* gene was reported in a single patient with LGMD and stroke (Lefeber *et al*., 2009), and mutations in dolichol kinase (*DOLK*; OMIM 610746) have been reported in children with severe cardiomyopathy with reduced α-dystroglycan glycosylation and elevated serum creatine kinase levels (Lefeber *et al*., 2011). Interestingly, a single case was found to have a primary dystroglycanopathy due to a homozygous missense mutation at the N-terminus of dystroglycan 1 (*DAG1*; OMIM 128239) (Hara *et al*., 2011). The phenotypic spectrum arising from mutations in these dystroglycanopathy genes is extremely wide and includes (i) forms of congenital onset weakness and severe structural brain abnormalities, including Walker–Warburg syndrome (OMIM 236670; Walker, 1942; Warburg, 1971), muscle–eye–brain disease (OMIM 253280; Raitta *et al*., 1978) and Fukuyama congenital muscular dystrophy (OMIM 253800; Fukuyama, 1960); (ii) forms with congenital onset of weakness ranging from absent to severe brain involvement, including congenital muscular dystrophy type 1C (MDC1C; OMIM 606612) (Brockington *et al*., 2001a) and type 1D (MDC1D; OMIM 608840) (Longman *et al*., 2003); and (iii) forms with later-onset limb-girdle weakness associated with mental retardation and microcephaly but without structural brain defects as seen in LGMD type 2K (LGMD2K; OMIM 609308) (Dincer *et al*., 2003), and the mildest variants with no brain involvement, such as in LGMD type 2I (LGMD2I; OMIM 607155) (Brockington *et al*., 2001b). Mutations in these genes mentioned above are responsible for 50–60% of the cases classified as dystroglycanopathy (Godfrey *et al*., 2007; Mercuri *et al*., 2009; Messina *et al*., 2010; Devisme *et al*., 2012). Using traditional positional cloning, the causative genes for the unsolved dystroglycanopathy cases had escaped discovery. Cirak *et al*. (2009) mapped a novel disease locus to chromosome 7p21 in a family with loss of α-dystroglycan glycosylation.

Recently we discovered that bi-allelic loss-of-function mutations in the isoprenoid synthase domain containing (*ISPD*) gene, which maps to chromosome 7p21, are a frequent cause of Walker–Warburg syndrome (Willer *et al*., 2012). We now report the identification of nine patients from seven families who have mutations in *ISPD*, with phenotypes ranging from congenital muscular dystrophy to LGMD. These families included the original family mapped to 7p21 (Cirak *et al*., 2009). Here we present the clinical, genetic and pathological features of the milder phenotypic spectrum related to mutations in *ISPD*.

Materials and methods

Subjects and clinical assessments

The study was approved by the Institutional Ethical Review Board of the University College London Institute of Child Health and Great Ormond Street Hospital in the UK, the Ethical Review Board of the University of Duisburg-Essen in Germany and the Human Use Committee at the University of Iowa. Informed consent was obtained

from the parents. The consent and local review board approval were in accordance with the UK10K project ethical framework (http://www.uk10k.org/ethics.html).

A three-generation family of Turkish origin with multiple loops of consanguinity demonstrating autosomal recessive inheritance was recruited (Supplementary Fig. 1). All three affected children and three unaffected siblings were examined, and serum creatine kinase levels were assessed in all siblings. The family was followed-up for >10 years, with the annual clinic visits at the University Children's Hospital Essen in Germany.

Forty-seven patients with the clinical and pathological diagnosis of a dystroglycanopathy were recruited at the Dubowitz Neuromuscular Centre at the Great Ormond Street Hospital London, UK. Genomic DNA was extracted from blood using standard procedures. In all patients, mutations in *POMT1*, *POMT2*, *POMGNT1*, *FKRP*, *FKTN* and *LARGE* were excluded by Sanger sequencing. Of these 47 cases, 14 underwent initial exome sequencing, and an additional 33 were Sanger sequenced after the discovery of the *ISPD* gene mutations. Apart from the three cases of the Turkish family reported in this study, all other 44 cases were unrelated.

Histology and immunohistochemistry

Immunohistochemical studies were performed as described previously (Dubowitz and Sewry, 2007). Muscle biopsies were obtained using standard techniques and mounted in optimal cutting temperature medium, and were then frozen by immersion in isopentane cooled in liquid nitrogen. Unfixed, frozen serial sections (7 μm) were incubated with primary antibodies for 1 h at room temperature, followed by three washes in phosphate buffered saline. Sections were then incubated with anti-mouse– or anti-rabbit–biotinylated IgG or IgM-biotinylated secondary antibodies (General Electric Healthcare, 1:200) for 30 min at room temperature. After washing, muscle sections were incubated with streptavidin conjugated to Alexa Fluor® 594 (Invitrogen, 1:1000) for 15 min at room temperature, and then washed and mounted using Hydromount mounting medium (National Diagnostics). Primary antibodies used were mouse monoclonal: α-dystroglycan IIH6 (clone IIH6C4, 1:200), α-dystroglycan VIA4-1 (Merck Millipore, 1:50), β-dystroglycan (clone 43dag1/8d5, Leica, 1:20), laminin-α2 (MAB1922 clone 5H2 Merck Millipore, 1:4000) to the 80-kDa C-terminal fragment, laminin-γ1 (LT3 Merck Millipore, 1:4000), laminin-β2 (gift from Dr Ulla Wewer, Clone S5F11, 1:500) (Wewer *et al*., 1997) and β-spectrin (Leica, 1:20), rat monoclonal laminin-α2 (clone 4H8–2 Alexis Corporation, 1:100) N-terminal fragment, goat polyclonal core α-dystroglycan (GT20ADG, 1:20). Sections were evaluated using a Leica DMR microscope interfaced to MetaMorph (Molecular Devices). Muscle biopsies from Cases 1, 2, 8 and 9 were processed and reported in the diagnostic pathology units elsewhere. The muscle biopsy from Case 5 was evaluated according to the methods described by Willer *et al*. (2012).

Western blot and immunoblot

Western blot of the available muscle biopsy specimens was performed as described by Brockington *et al*. (2010). The following primary antibodies were used for the western blot of the muscle biopsies from Cases 4 and 7: anti-mouse α-dystroglycan IIH6 (Merck Millipore, catalogue 05-593), α-dystroglycan VIA4-1 (Leica, 1:50) and anti-mouse β-dystroglycan (Leica). Further experimental details are outlined in the Supplementary material. The muscle biopsy of Case 5 was studied using wheat germ agglutinin-enriched muscle homogenates as described previously (Michele *et al*., 2002). Immunoblots were done on polyvinylidene difluoride membranes as described earlier (Michele *et al*., 2002). The following antibodies were used for Case 5: the monoclonal antibodies to the fully glycosylated form of α-dystroglycan (IIH6 and VIA4) (Ervasti and Campbell, 1991) and α-dystroglycan (AP83) (Duclos *et al*., 1998). Shp5 (core-α-DG) from sheep antiserum was raised against the dystrophin–glycoprotein complex in its entirety and purified against a hypoglycosylated full-length α-DG–human IgGFc fusion protein (Kunz *et al*., 2001). Blots were developed by horseradish peroxidase enhanced chemiluminescence (Pierce).

Exome sequencing and data processing

Genomic DNA (1–3 μg) was sheared to 100–400 bp using a Covaris E210 or LE220 ultarsonicator. Sheared DNA was subjected to Illumina paired-end DNA library preparation and enriched for target sequences (Agilent Technologies; Human All Exon 50 Mb-ELID S02972011) according to the manufacturer's recommendations (Agilent Technologies; SureSelectXT Automated Target Enrichment for Illumina Paired-End Multiplexed Sequencing). Enriched libraries were sequenced using the HiSeq™ platform (IIIumina) as paired-end 75-bp reads according to the manufacturer's protocol. Sequencing reads that failed quality filtering were removed using the Illumina Genome Analyser Pipeline. The mean coverage of the exomes was 74 times with the descriptive exome, and statistical data are presented in Supplementary Table 1.

The Burrows–Wheeler Aligner (Li and Durbin, 2009) was used for alignment to the human reference genome build UCSC hg19, followed by the removal of polymerase chain reaction (PCR) duplicates using Picard (http://picard.sourceforge.net). The variant calling was performed in target ± 100-bp regions. For the variant calling, SAMtools (version 0.1.17) (Li *et al*., 2009) and Genome Analysis Toolkit (GATK)-Unified Genotyper (version 1.1-5) (McKenna *et al*., 2010) were used. Base quality recalibration and indel realignment were done with the help of GATK (DePristo *et al*., 2011). For each exome sample, variant sites (single nucleotide polymorphisms and indels) are called using the GATK-Unified Genotyper, and marked up with single nucleotide polymorphism database (dbSNP)132 rs-ids, GATK variant filtration applied (soft filter), including an indel mask consisting of 1000 Genomes pilot indels. Variants were assigned to quality tranches by GATK. The variants called by each of the callers were filtered separately using vcf-filter. For each sample, the resulting gatk.vcf and mpileup.vcf files were merged using vcf-isec. GATK annotations are preferred if sites are in both call sets. The variant calls were annotated using vcf-annotate for the following information: earliest version of dbSNP containing this call, dbSNP 132 rsIDs and 1000 Genomes population allele frequencies. The 1000 Genomes frequencies are taken from the June 2011 data release (http://www.1000genomes.org/data). Additionally, a number of functional scores were annotated to aid the filtering of variants. Further details of the variant calling and annotation procedures are listed in the Supplementary material.

Variant filtering

We used an in-house software to dynamically filter candidate variants on the basis of the autosomal recessive inheritance. Depending on the pedigree structure, we looked for either homozygous or two functional heterozygous changes in the same gene. The filtering at the *ISPD* locus was stringent, excluding the following variants: present in dbSNP132, present in 1000 Genomes, synonymous and other non-coding variants apart from essential splice site changes and not present in remaining UK10K rare disease cohort (322 exomes at the time of the analysis). None of the variants were present in the National Heart, Lung, and Blood Institute (NHLBI) Exome Sequencing Project database.

Copy number analysis

We used ExomeDepth (Plagnol *et al*., 2012, available at http://cran.r-project.org/) to fit a robust beta-binomial model to the read count data. By comparing read count between the test sample and additional exome samples from the same batch, this software predicts the expected read count. Deviations from this expectation are used to call copy number variants. ExomeDepth was run on all 14 cases who were whole-exome sequenced.

Experimental copy number validation

Quantitative fluorescent PCR analysis was performed as described previously (Yau *et al*., 1996). A single quantitative fluorescent PCR assay was designed to determine the copy number of exons 2, 3, 4, 5, 6, 7, 8, 9 and 10 of the *ISPD* gene by amplifying nine amplicons in a single 20-µl reaction using 6-FAM (Life Technologies) labelled forward primers and non-labelled reverse primers (primers and amplification conditions available on request). Fluorescent amplicons were analysed on an ABI 3730 DNA Analyzer (Applied Biosystems), and the data were then analysed with GeneMarker (SoftGenetics). The relative copy number of each exon was determined using dosage quotients as previously described (Yau *et al*., 1996).

Sanger sequencing

All exons and 50 bp of the flanking introns of the *ISPD* gene were sequenced from genomic DNA extracted from blood using standard protocols. PCR products were amplified using standard techniques and purified for sequence analysis with ExoI/shrimp alkaline phosphatase. Bi-directional fluorescent sequencing analysis was performed by the UCL genomic services using BigDye® v.1.1 Cycle Sequencing Kits (Applied Biosystems), which were analysed on an ABI 3730XL DNA Analyzer (Applied Biosystems) after purification using ethanol precipitation. Primer sequences are available on request. Each sequence was analysed visually using the Lasergene Seqman (DNASTAR) software.

Results

Clinical findings

We have identified nine cases from seven families with phenotypes milder than Walker–Warburg syndrome and *ISPD* mutations. Clinical features are summarized in Table 1, while a more detailed clinical case description is provided in the Supplementary material.

Cases 1, 2, 3, 5 and 7 have an LGMD-like phenotype without brain involvement (Fig. 1). Each of these five patients presented in early childhood with difficulty in walking and evidence of a Gowers' sign. Case 3 is currently 4 years old and ambulant, but with proximal weakness and evidence of a Gowers' sign. In Cases 1, 2, 3, 5 and 7, gross motor function improved until the age of ~4 years, and all acquired the ability to climb stairs. Progression of proximal muscle weakness, however, led to loss of independent ambulation by the age of 12 years in Cases 1, 2 and 7. In Case 5 (Fig. 1), hypotonia was noted during the first year of life, but the subsequent disease course has been LGMD-like, making the overall phenotype intermediate congenital muscular dystrophy/LGMD-like. Generalized muscle hypertrophy was common, which included tongue hypertrophy in Cases 1 and 2 (Fig. 1). Case 8 is currently 10 years old and has a milder LGMD phenotype with learning difficulties. She is fully ambulant and can run slowly despite proximal muscle weakness. Case 4, currently aged 7 years, has a congenital muscular dystrophy phenotype without brain involvement. She never achieved independent walking or standing, but can use a self-propelling wheelchair and bottom shuffles.

In terms of cardiopulmonary involvement, a mild decrease in heart function with a fractional shortening of 27% was documented in Case 1 at the age of 19 years, for which isoprolol was started. The patient's forced vital capacity was almost normal, at 85% predicted. Case 2 had mildly reduced left ventricular heart function noted at the age of 12, for which treatment with captopril was started. Case 7 developed nocturnal hypoventilation at the age of 18 years. Her ECG showed a reduced left ventricular ejection fraction of 45%. Case 9 developed respiratory insufficiency at the age of 23 years, with a forced vital capacity of 49% predicted. Her ECG revealed normal heart function.

Cases 6 and 9 (Fig. 1) have overlapping clinical features between congenital muscular dystrophy and LGMD and, for this reason, will be presented in more detail. Both presented in the first year of life with hypotonia and eye and brain involvement (with structural cerebellar and brainstem MRI abnormalities), but followed a relatively mild LGMD-like disease course. As their presenting symptoms were that of feeding and eye movement problems without weakness, this suggests that their early presentations were secondary to the CNS brain involvement, and not the severity of their muscle involvement. Case 6 is a boy aged 8.5 years. He presented at 6 months with a squint and was subsequently diagnosed with oculomotor apraxia, with difficulties in initiating saccades, a choroidal coloboma and severe myopia. Multiple cerebellar cysts were seen on brain MRI, and creatine kinase was >1500 IU/l. A muscle biopsy performed at 16 months identified a dystrophic process. From the developmental perspective, he sat with support at 8 months and started to walk at 15 months. At the age of 4 years, his head circumference was 50 cm (9th percentile), and he had evidence of axial weakness with subgravity neck and hip girdle power, but antigravity strength in the remaining muscles. He rose from the supine position with a Gowers' sign. Ophthalmological examination revealed apraxic ocular movements and head thrusts, nystagmus at the extremes of gaze and an intermittent, alternating convergent squint. At his last clinical evaluation at the age of 7 years, he demonstrated further improvements. He stood with a lordotic posture and evidence of mild scapular winging. He rose from the floor in 1.4 s and had a waddling-type gait. Currently he is attending mainstream school with average academic achievements. Case 9 (Fig. 1) is a female who presented at birth with transient hypotonia and poor feeding. At 6 months of age, she was diagnosed with severe myopia and strabismus. She made rapid motor progress, and was able to sit at 6 months and walk at 18 months. At the age of 10 years, she lost the ability to rise from the floor. She is normocephalic. Her formal cognitive function was within the normal range (IQ of 89). At the age of 20, the examination showed paresis of superior oblique

Table 1 Clinical summary

Case	Age/sex	Phenotype classification	Serum creatine kinase (IU/l)/age	Age of onset/ symptoms	Age of maximal motor ability/ motor function	Current motor ability	Pattern of muscle weakness	Brain MRI	Eye involvement	Other features/age
1	21 years/F	LGMD-no MR	2000/1 month	1.5 years/ frequent falls	3–4 years/ managing stairs	Non-ambulant since 12 years	Proximal, DMD-like	Normal	No	Cardiac: FS= 27%/ 19 years
2	14 years/F	LGMD-no MR	1800/14 months	1.5 years/ Gowers' sign	3–4 years/ managing stairs	Non-ambulant since 12 years	Proximal, DMD-like	Normal	No	Cardiac: mildly reduced LV function/12 years
3	4 years/F	LGMD-no MR	9097/4 years	2 years/ Gowers' sign	4 years/ managing stairs	Fully ambulant	Proximal, DMD-like	ND	No	NA
4	7 years/F	CMD-no MR	6000/16 months	1 years/not standing	5–6 years/ standing frame	Sitting	Proximal	ND	No	NA
5	11 years/F	CMD/LGMD-no MR	5000/1 years	1 years/reduced movement in legs	4–5 years/ managing stairs	Non-ambulant	Proximal	Normal	No	NA
6	8.5 years/M	LGMD-CRB[a]	1500/6 months	0.5 years/ oculomotor apraxia	7 years/ running	Fully ambulant	Proximal	Cerebellar cysts	Severe myopia; oculomotor apraxia	NA
7	18 years/F	LGMD-no MR	4000/3.5 years	3.5 years/ Gowers' sign	5 years/ managing stairs	Non-ambulant since 12 years	Proximal, DMD-like	Normal	No	Cardiac: EF= 45%/ 18 years Respiratory: nocturnal hypoventilation/18 years
8	10 years/F	LGMD-MR	5849/6 years	3 years/walking difficulties	10 years/ running	Fully ambulant	Proximal	Normal	No	Cognitive: moderate learning difficulties
9	23 years/F	LGMD-CRB[a]	719/23 years	0.5 years/severe myopia and strabismus	5 years/ managing stairs	Standing, few steps with assistance	Proximal	Brainstem hypoplasia; cerebellar hypoplasia; fourth ventricle dilatation	Severe myopia; strabismus	Respiratory: FVC= 49%/23 years Feeding: mild swallowing difficulties/23 years

a Newly proposed dystroglycanopathy category: limb-girdle muscular dystrophy with cerebellar involvement (LGMD-CRB).
CMD = congenital muscular dystrophy; DMD = Duchenne muscular dystrophy; EF = ejection fraction; FS = fractional shortening; FVC = forced vital capacity; LV = left ventricle; MR = mental retardation; NA = not applicable; ND = not done.

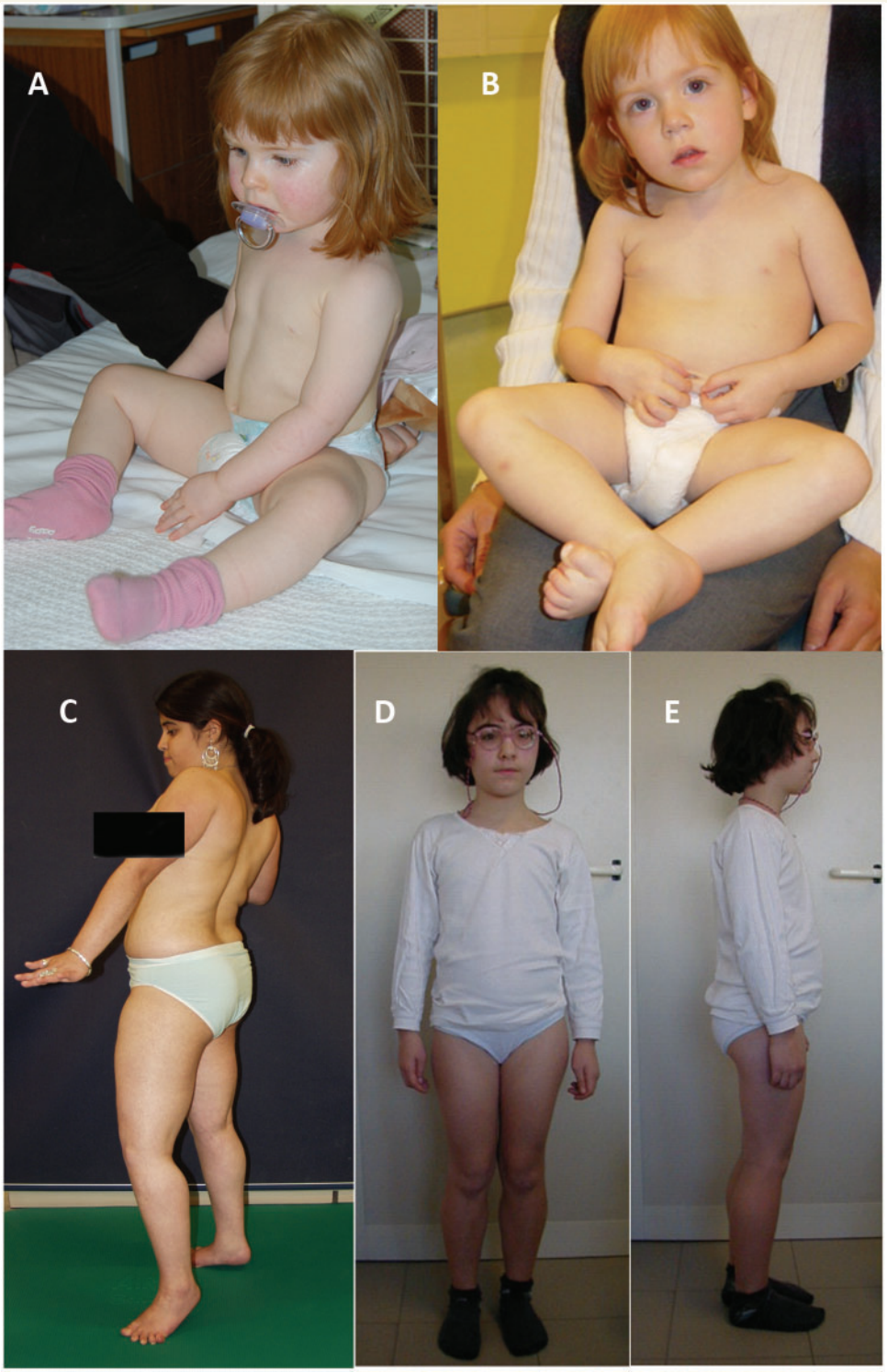

Figure 1 Clinical phenotype. *Top:* The clinical phenotype of *ISPD*-related muscular dystrophy in early childhood with pseudohypertrophy of lower limb muscles (**A** and **B**). *Bottom:* The disease at a later stage with marked pseudohypertrophy and ankle contractures (**C**, **D** and **E**). (**A**) Case 4 at 1.5 years, (**B**) Case 5 at 2.5 years, (**C**) Case 1 at 15.5 years, (**D** and **E**) Case 9 at 8 years.

muscles and abducens muscles and strabismus without clear oculomotor apraxia. She also had myopia and buphthalmos. Currently, at 23 years of age, she can take a few steps indoors with assistance only and has been experiencing mild swallowing difficulties.

Brain imaging

Brain imaging was available for Cases 1, 2, 5, 6, 7, 8 and 9. Brain magnetic resonance imaging (MRI) of Case 6 performed at 1 year showed multiple cerebellar cysts and supratentorial white matter

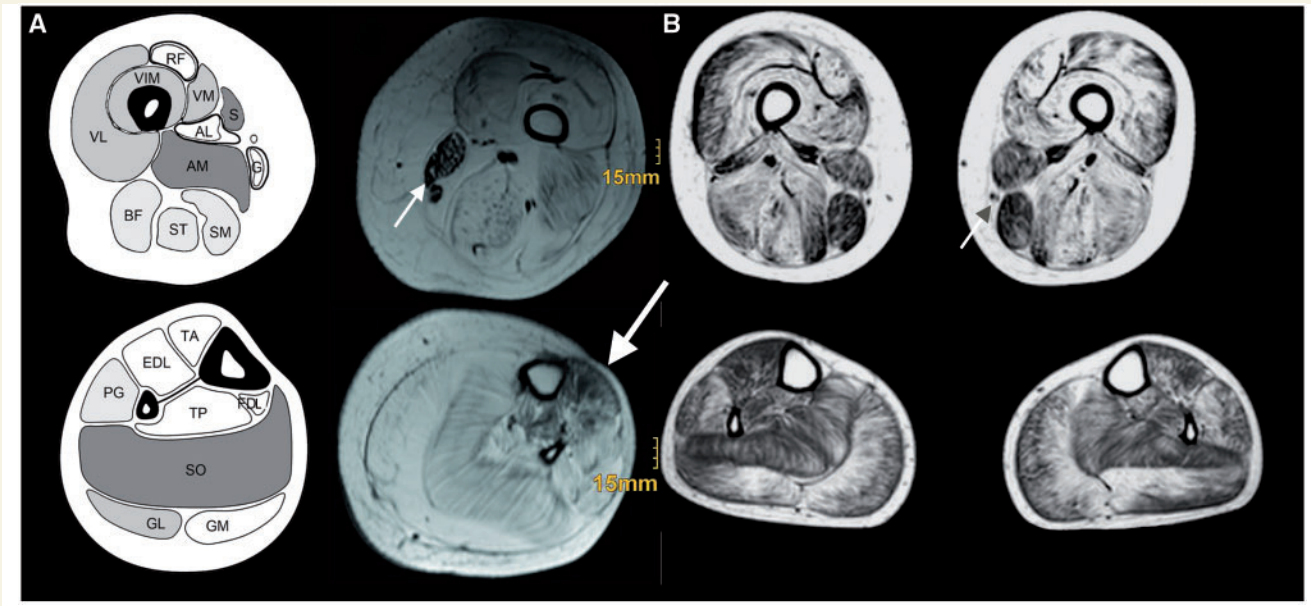

Figure 2 Muscle MRI. (**A**) The T_1-weighted muscle MRI of the thigh and calf of Case 1 at 19.5 years of age. (**B**) The T_1-weighted muscle MRI of the thigh and calf of Case 9 at 20 years of age. There is sparing of sartorius and gracilis muscles (small arrows) in the thigh in both patients and sparing of the tibialis anterior muscle more visible in Case 1 (large arrow). The differential degree of fatty fibrous replacement is in concordance with the clinical severity with regards to ambulation, as Case 1 lost ambulation at 13 years, and Case 9 can still take a few steps with assistance only at age 23 years. AL = adductor longus; AM = adductor magnus; BF = biceps femoris; EDL = extensor digitorum longus; FDL = flexor digitorum longus; G = gracilis; GL = gastrocnemius lateralis; GM = gastrocnemius medialis; PG = peroneal group; RF = rectus femoris; S = sartorius; SM = semi-membranosus; SO = soleus; ST = semi-tendinosus; TA = tibialis anterior; TP = tibialis posterior; VL = vastus lateralis; VM = vastus medialis.

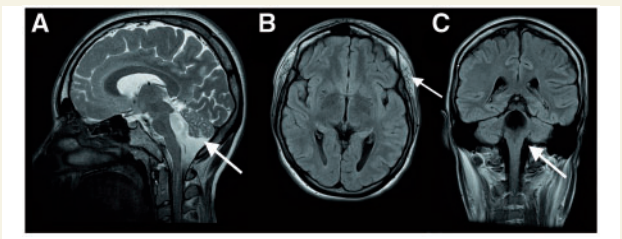

Figure 3 Brain MRI of Case 9 performed at 21 years of age, revealing brainstem hypoplasia, cerebellar hypoplasia and dilated fourth ventricle. (**A**) Sagittal T_2-weighted image of the brain demonstrating brainstem hypoplasia, cerebellar hypoplasia and dilated fourth ventricle (arrow). (**B**) Axial T_1-weighted image of the brain, revealing a normal appearance of the cerebral hemispheres. Interestingly, the temporalis muscles show some fibro-fatty changes (arrow). (**C**) Coronal T_1-weighted image of the brain demonstrating dilatation of the fourth ventricle (arrow).

changes (not shown). Case 9 had a brain MRI performed at 21 years that demonstrated brainstem hypoplasia, cerebellar hypoplasia, dilated fourth ventricle and evidence of bilateral buphthalmos (Fig. 3). The findings of the brain MRIs of the remaining cases were normal.

Muscle imaging

Muscle MRI was performed in Case 2 at 19.5 years and Case 9 at 20 years. Images revealed noticeable sparing of sartorius and gracilis muscles in both cases; sparing of the tibialis anterior muscle was more evident in Case 1 (Fig. 2). The degree of fibro-fatty replacement of muscle appeared to be concordant with the clinical severity.

Muscle biopsy findings

Quadriceps muscle biopsies were performed in all cases except in Case 3. Routine histochemical studies revealed variable degrees of dystrophic features in all biopsies evaluated that included variation in fibre size, increased fibrosis and evidence of myonecrosis and regeneration. Immunolabelling with the α-dystroglycan antibodies (IIH6 and VIA4-1) was negative or severely reduced (Table 2). However, there was evidence of preserved expression of α-dystroglycan using the core antibody (GT20ADG) in those biopsies in which this analysis could be performed (Cases 4, 6 and 7) (Fig. 4). Laminin α-2 expression was reduced in all cases except in Case 5. Laminin α-2 immunolabelling was reduced in some cases (data not shown), whereas β-dystroglycan (Fig. 4) was generally well preserved (immunolabelling was slightly uneven on some fibres in Case 7, but no significant reduction was detected on immunoblots) (Supplementary Figs 5 and 6).

Immunoblot analysis

Because of sample availability, a western blot analysis was possible only in Cases 4, 5 and 7 (Supplementary Figs 5 and 6). The wheat

Table 2 Mutations and pathology

Case[a]	Age (years) at time of biopsy	Laminin α-2	α-dystroglycan (glycoepitope IIH6)	α-dystroglycan (core 20)	Genetic Screening technique[b]	Variant 1[c]	Variant 2[c]
1	4	Reduced on many fibres	Negative	ND	Sanger	Exon 8: c.1114_1116del; p.(Val372del)	Exon 8: c.1114_1116del; p.(Val372del)
2	1.5	Reduced on many fibres	Negative	ND	Sanger	Exon 8: c.1114_1116del; p.(Val372del)	Exon 8: c.1114_1116del; p.(Val372del)
3	F	ND	ND	ND	Sanger	Exon 8: c.1114_1116del; p.(Val372del)	Exon 8: c.1114_1116del; p.(Val372del)
4	2	Reduced	Traces	Mild reduction	Exome	Exon 2: c.446C>T; p.(Pro149Leu)	Exon 3: c.643C>T; p.(Gln215*)
5	1	Positive (80-kDa epitope); slight reduction 300-kDa epitope	Many fibres negative (VIA4-1– traces)	Positive	Exome	Exon 8: c.1114_1116del; p.(Val372del)	Exon 9: Het c.1183A>T; p.(Arg395*)
6	1.3	Reduced	Many fibres negative	Mild reduction	Exome/ Sanger	Exon 1: c.2T>G; p.(M1_R59del)	Exon 2: c.377G>A; p.(Arg126His)
7	11	Reduced on many fibres	Traces	Positive, mild reduction on some fibres	Exome/ Sanger	Exon 1: c.157G>A; p.(Ala53Thr)	Exon 9: c.1183A>T; p.(Arg395*)
8	6	Marked reduction on Immunoblot	Traces	ND	Sanger	Exon 1: c.53dup; p.(Ser19Glufs*97)	Exon 3: c.677A>G; p.(Tyr226Cys)
9	5	ND	Negative	ND	Exome	Exon 6 to 8 duplication; c.836-?_1119+?dup; p.Val374Rfs*8	Exon 6 to 8 duplication; c.836-?_1119+?dup; p.Val374Rfs*8

a Cases 1, 2 and 3 are affected individuals from the same family. Cases 4 to 9 are all unrelated individuals.
b Screening technique used to originally identify mutation: Exome = Next Generation Sequencing Exome; Sanger = dideoxy fluorescent sequencing; Exome/ Sanger = indicate both techniques required to detect both mutations. Exon 1 of *ISPD* was not covered by the exome data and therefore additional Sanger sequencing of exon 1 was necessary.
c Mutation nomenclature follows the recommended guidelines (www.hgvs.orf/mutnomen) with the nucleotide numbering based on GenBank reference sequence NM_001101426.3. Nucleotide numbering denotes the adenosine of the annotated translation start codon as nucleotide position +1.

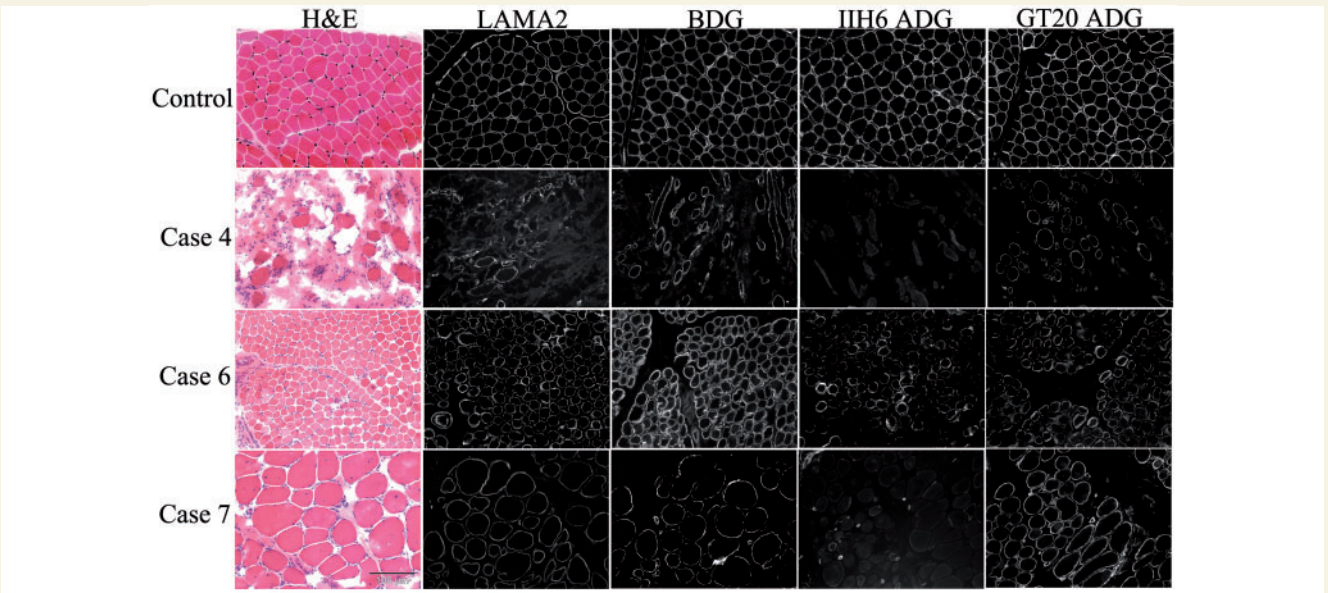

Figure 4 Immunohistochemistry of muscle biopsies from cases with *ISPD*-related muscular dystrophy. Unfixed frozen sections of quadriceps muscle biopsies from a control and three *ISPD* patients (Cases 4, 6, and 7) stained with haematoxylin and eosin (H & E) and immunolabelled with antibodies against laminin-α2 (LAMA2), β-dystroglycan (BDG), the glycosylated epitope of α-dystroglycan (IIH6 ADG) and the core protein of α-dystroglycan (GT20 ADG). Laminin-α2 immunostaining was reduced in all *ISPD* cases. Although expression of β-dystroglycan was similar to the control (see text), glycosylated α-dystroglycan immunolabelling was absent in Cases 4 and 7 and severely reduced in Case 6. Core α-DG (GT20ADG) was well preserved in all the cases.

germ agglutinin-enriched lysate from the muscle biopsy of Case 5 showed α-dystroglycan hypoglycosylation as suggested by the lack of binding affinity to the glycoepitope-specific antibodies IIH6 and VIA4-1. Western blot analysis of skeletal muscle of Cases 4 and 7 showed a profound reduction in α-dystroglycan expression using the IIH6 antibody, whereas β-dystroglycan expression was normal.

Genetics

All listed mutations are named according to reference sequence NM_001101426.3 (Fig. 5), corresponding to the long isoform of *ISPD,* which has 10 exons. Exon 3 of this long isoform is not present in the other short isoform (NM_001101417.3). Exome sequencing in Case 4 showed the following *ISPD* mutations at the heterozygous state: g.chr7: 16255759 T>A, c.446 C>T, causing p.Pro149Leu, which is located in exon 2 and g.chr7:16445774 G>A, c.643 C>T, p.Gln215* in exon 3. Exome sequencing in Case 5 showed a heterozygous premature stop codon mutation in exon 9: g.chr7:16255759 T>A, c.1183A>T, p.Arg395* and a heterozygous in-frame triplet deletion in exon 8: g.chr7:16298017 AAAC>A, c.1114-1116delGTT, leading to a single amino acid deletion p.Val372del. Exome sequencing in Case 6 showed a heterozygous missense mutation in exon 2: g.chr7:16445843 C>T, which is c.377G>A, leading to p.Arg126His. Interestingly, the second compound heterozygous mutation affecting the start codon in exon 1 c.2T>G, leading to p.M1_R59del or p.M1?, was identified only by Sanger sequencing, as exon 1 was not covered by the exome sequencing.

Exome sequencing in Case 7 revealed a heterozygous stop mutation in exon 9: g.chr7:16255759 T>A, leading to c.1183 A>T and causing p.Arg395*. The second compound heterozygous mutation was found by Sanger sequencing to be c.157G>A causing p.Ala53Thr located in exon 1. All *ISPD* mutations found by exome sequencing were confirmed by Sanger sequencing.

Following the discovery of mutations in the *ISPD* gene by whole exome sequencing, the original family that was mapped to chromosome 7p21 was screened for mutations in all 10 exons of the *ISPD* gene by Sanger sequencing. All the affected individuals in this family (Cases 1, 2 and 3) were found to have inherited a homozygous 3-bp deletion in exon 8 resulting in a single amino acid deletion (c.1114-1116delGTT; p.Val372del). The mutation was found to be co-segregating with the phenotype. In the remaining cases, we identified one patient (Case 8) with a frameshift mutation (c.53dupT) in exon 1 and a missense mutation in exon 3 c.677A>G (p.Tyr226Cys). The heterozygous carrier status of the parents demonstrating the expected phase for an autosomal recessive inheritance was confirmed in all families except in the family of Case 6, as parental DNA was not available.

A read depth copy number analysis (R package ExomeDepth, Plagnol *et al*., 2012) of the exome sequence from Case 9 detected double the number of expected reads in a 40 916 kb region [chr7:16276936–16317852 (UCSC hg19)] involving exons 6, 7 and 8 of the *ISPD* gene (Supplementary Fig. 2). Quantitative fluorescent PCR analysis of genomic DNA confirmed that *ISPD* exons 6, 7 and 8 were homozygously duplicated in Case 9, resulting in an out-of-frame duplication (Supplementary Fig. 4) and that both her parents were carriers of the mutation (data not shown).

Discussion

Functional glycosylation defects of α-dystroglycan represent a major pathological subgroup of congenital and LGMDs. These so-called dystroglycanopathies range from a lethal clinical variant

Figure 5 ISPD protein and mutations. The domain structure of the ISPD protein is illustrated and the corresponding exons are shown. The darker region represents the active functionally conserved CDP-ME domain (V47–A273). Mutations found in a compound heterozygous state are connected with a horizontal line. The small-sized horizontal bars represent the number of observed alleles. *Bottom:* The conservation of the missense mutations (marked with bold letters) within the vertebrates [*Homo sapiens* NP_001094896.1; *Pan troglodytes* (XP_003318374.1) 99% amino acid identity; *Macaca mulatta* (XP_001105001.2) 94% amino acid identity; *Bos taurus* (XP_002686725.1) 81% amino acid identity; *Canis lupus* familiaris (XP_003431914.1) 84% amino acid identity; *Rattus norvegicus* (NP_001008387.1) 73% amino acid identity; *Mus musculus* (NP_848744.1) 74% amino acid identity; *Gallus gallus* (XP_418693.2) 66% amino acid identity; *Xenopus tropicalis* (NP_001016240.1) 60% amino acid identity; *Danio rerio* (NP_001071270.1) 47% amino acid identity].

of Walker–Warburg syndrome with cerebral and ocular involvement to milder forms of adult-onset LGMD such as LGMD2I (Godfrey *et al*., 2007). Although each of the eight known genes that code for putative or demonstrated glycosyltransferases or proteins involved in the glycosylation of α-dystroglycan could in theory cause each of these clinical variants, there has been a marked difference in frequency and clustering of phenotypes for certain known genes so far. Mutations in *FKRP* are the most common cause of dystroglycanopathy in the UK (Mercuri *et al*., 2003, 2009; Poppe *et al*., 2003) and can cause the entire spectrum of dystroglycanopathy phenotypes (Brockington *et al*., 2002; Brown and Winder, 2012; Devisme *et al*., 2012). Other genes such as *POMGNT1*, *POMT1* and *POMT2* are mostly responsible for phenotypes with CNS involvement (Mercuri *et al*., 2009; Messina *et al*., 2010; Brown and Winder, 2012; Devisme *et al*., 2012). The *DPM3* and *DOLK* genes, which represent an overlapping group with *N*-glycosylation disorders and dystroglycanopathies, are rare, as only a handful of cases have been described to date (Lefeber *et al*., 2009, 2011; Brown and Winder, 2012). The genetic aetiology of this group is indeed diverse, and ~50% of the cases with dystroglycanopathy remain unsolved (Wewer *et al*., 1997; Mercuri *et al*., 2009). After the discovery of bi-allelic loss-of-function mutations in *ISPD* causing Walker–Warburg syndrome (Roscioli *et al*., 2012; Willer *et al*., 2012), we can now describe the full spectrum of phenotypes caused by recessive mutations in *ISPD* including a quite common milder allelic LGMD phenotype. The spectrum of the phenotypes ascertained in this study ranges from cases with congenital muscular dystrophy without CNS involvement (Case 4), milder cases with LGMD without CNS involvement (Cases 1, 2, 3, 5 and 7) (Fig. 1) and a rather unusual and novel phenotype with relatively mild skeletal muscle weakness manifesting as a LGMD and structural brain involvement affecting predominantly the subtentorial structures (Cases 6 and 9) (Fig. 1), confirming once again the preferential involvement of subtentorial structures in dystroglycanopathies (Clement *et al*., 2008). This phenotype is in contrast to LGMD2K, which is associated with microcephaly and mental retardation (Lommel *et al*., 2010), a phenotype that Case 8 in our series resembles. As an LGMD phenotype with structural cerebellar involvement has not been reported in any of the remaining dystroglycanopathies, this combination of features appears to be highly evocative of an *ISPD*-related muscular dystrophy. We suggest the use of the term 'limb-girdle muscular dystrophy with cerebellar involvement' (LGMD-CRB) to describe these patients. This term could be added to the recently proposed classification of dystroglycanopathies (Godfrey *et al*., 2011).

As in other dystroglycanopathies, *ISPD*-related disease is progressive, with most cases with LGMD losing ambulation in their early teenage years, thus following a Duchenne muscular dystrophy-like path. In several patients, there was muscle pseudohypertrophy, including the tongue. Respiratory and cardiac functions also demonstrated decline, resembling that reported for other dystroglycanopathies (Mercuri *et al*., 2003; Murakami *et al*., 2006; Bourteel *et al*., 2009; Lefeber *et al*., 2011; Yilmaz *et al*., 2011). Therefore, regular surveillance of heart function by ECG and respiratory function by regular overnight polysomnography is required in *ISPD*-related muscular dystrophy. Muscle MRI shows replacement with fat and connective tissue in the lower limbs with sparing of the semitendinosus and gracilis muscles in the thighs and the tibialis anterior muscle in the calves. Interestingly, the gracilis muscle is also spared in *FKRP*-related LGMD2I (Bourteel *et al*., 2009).

From the histopathological perspective, all cases show substantially reduced IIH6 or VIA4-1 labelling, indicating the loss of functional α-dystroglycan glycosylation. Using immunocytochemistry, there were no clear differences in IIH6 staining between severe and milder phenotypes in the majority of cases. The lack of correlation between severity of skeletal muscle involvement and loss of the IIH6 epitope on immunocytochemistry and immunoblot (even after wheat germ agglutinin enrichment, Case 5) is quite striking in *ISPD*-related muscular dystrophy. Variable correlations between clinical phenotype and IIH6 content in skeletal muscle have been reported for mutations in other genes such as *FKRP* and *FKTN* (Jimenez-Mallebrera *et al*., 2009), while there appears to be a better correlation for *POMT1*-, *POMT2*- and *POMGNT1*-related dystroglycanopathies (Jimenez-Mallebrera *et al*., 2009; Lommel *et al*., 2010). This poor correlation (i.e. apparent severe depletion of IIH6 epitope also in patients with relatively milder variants) may be due to the fact that there is some laminin-binding activity on α-dystroglycan owing to other glycans that are not recognized by IIH6 (McDearmon *et al*., 1998, 2001, 2003, 2006; Stalnaker *et al*., 2010, 2011). Our genetic data (Fig. 5) demonstrate a good genotype–phenotype correlation in the *ISPD*-related muscular dystrophy. We have previously shown (Willer *et al*., 2012) that bi-allelic loss-of-function mutations cause a Walker–Warburg syndrome phenotype. Compound heterozygosity of a missense mutation and a loss-of-function mutation affecting one of the first five exons of *ISPD* results in a congenital muscular dystrophy phenotype (Case 4), LGMD-CRB phenotype (Case 6) or a LGMD phenotype with mental retardation (Case 8), because the first five exons of *ISPD* contain the functional conserved 4-diphosphocytidyl-2-methyl-D-erythritol synthase (CDP-ME) domain. The cases with milder LGMD without brain involvement have either a homozygous in-frame deletion of a single amino acid in exon 9 (p.V372del) (Cases 1, 2 and 3) or are compound heterozygous for a mild mutation and a stop mutation in exon 9 (Cases 5 and 7). Mutations in other domains could also alter the function of ISPD substantially, as a homozygous stop mutation p.Glu396* has been reported to cause a Walker–Warburg syndrome phenotype (Roscioli *et al*., 2012). The effect of the homozygous duplication of exons 6, 7 and 8 in Case 9 is also interesting. We predicted that the open reading frame would be translated until exon 8 and followed by a frameshift in exon 9, which could lead to a truncated ISPD protein (Val374Rfs*8). The mild phenotype in this patient is surprising and could be accounted for by a number of different mechanisms: (i) there could be a splicing aberration leading to the production of reduced levels of an in-frame message; (ii) the truncated protein could be partly active, as the CDP-ME containing exons of *ISPD* are translated; and (iii) there could be incomplete nonsense-mediated decay related to the mutation occurring towards the 3′ end of the gene. The question that remains is how these dystroglycanopathy phenotypes might be explained by the putative function of ISPD. In eubacteria, green algae and chloroplasts of higher plants, ISPD

orthologues are part of the methylerythritol pathway. This pathway contains the CDP-ME domain and catalyzes the third step in the alternative (non-mevalonate) pathway of isopentenyl diphosphate biosynthesis (isoprenoid precursor). The formation of 4-diphosphocytidyl-2C-methyl-D-erythritol from cytidine triphosphate and 2C-methyl-D-erythritol 4-phosphate is also called cytidyltransferase activity. This mevalonate-independent pathway uses pyruvate and glyceraldehyde 3-phosphate as starting materials for production of isopentenyl diphosphate and occurs in a variety of bacteria, archaea and plant cells but is absent in mammals, which suggests that ISPD must have a different function(s) in humans. The mechanism by which *ISPD* mutations lead to a reduction of α-dystroglycan glycosylation is not well understood. Apart from the CDP-ME domain, ISPD also contains and belongs to the glycosyltransferase-A family (Breton *et al*., 2006). Interestingly, *LARGE* also belongs to this glycosyltransferase-A family. The function of LARGE has been partly elucidated; it acts as a bi-functional glycosyltransferase, with both xylosyltransferase and glucuronyltransferase activities, attaching repeating units of [-3-xylose-α1,3-glucuronic acid-β1-] to α-dystroglycan (Inamori *et al*., 2012). Considering that there are also some prokaryotes that lack the methylerythritol pathway and contain homologous enzymes such as TarI in *Streptococcus pneumonia*, which synthesizes activated CDP-ribitol (Baur *et al*., 2009; Roscioli *et al*., 2012), one could hypothesize that in vertebrates ISPD activates nucleotide sugar building blocks for complex α-dystroglycan glycosylation or even that it could have complex glycosyltransferase activity similar to LARGE. However, the experimental evidence reported in our recent study (Willer *et al*., 2012) suggests that in patients with *ISPD*-deficient Walker–Warburg syndrome, *O*-mannosylation was strongly impaired and subsequently the *O*-mannosyl phosphorylation and LARGE-dependent hyperglycosylation were absent (Willer *et al*., 2012). This indicates the pivotal role for ISPD in the initial step of the *O*-mannosylation of α-dystroglycan.

Mutations in *ISPD* appear to be relatively common; in our previous population study (Willer *et al*., 2012), we evaluated 92 patients with dystroglycanopathy after exclusion of *FKRP*, and the most frequent mutations found were in *POMT1* and *POMT2* (8.6% each). Here we have screened 47 cases, and 7 of 44 (16%) non-familial cases have mutations in *ISPD*. We recently reported that 30% of the Walker–Warburg syndrome cohort and 11% of the dystroglycanopathy cohort (Willer *et al*., 2012) have *ISPD* mutations, similar to another report on Walker–Warburg syndrome (Roscioli *et al*., 2012). The *ISPD* gene also appears to be frequently affected by copy number variations (Willer *et al*., 2012); therefore, testing for copy number variations in *ISPD* will be essential in the diagnostic evaluation of patients with dystroglycanopathy.

In conclusion, *ISPD* mutations are a common cause of secondary dystroglycanopathy with a phenotypic spectrum ranging from Walker–Warburg syndrome to LGMD. As the laminin-binding glycoepitope is almost undetectable in most of the cases with *ISPD*-related muscular dystrophy, the elusive function of ISPD must have a pivotal role for functional α-dystroglycan glycosylation. Uncovering of the ISPD function will help to decipher the glycosylation pathway of α-dystroglycan.

Acknowledgements

The authors thank Dr Lucy Feng and Darren Chambers for the excellent processing of muscle biopsy specimen and muscle biopsy images. They thank Prof Knut Brockmann, Dr Lars Klinge, Dr Adnan Manzur and Dr Stephanie Robb for providing clinical information, and Dr Emma Clement and Dr Caroline Godfrey for their earlier work on the dystroglycanopathy cohort. The NSCT Newcastle Biopsy Service is also acknowledged for providing the pathology report of Case 8.

Funding

The authors are grateful to the Wellcome Trust funded UK10K consortium for making this study possible. A.R.F. is a Muscular Dystrophy Campaign Fellow. F.M. is supported by the Great Ormond Street Children's Charity and the GOSH Biomedical Research Centre. This study was supported by the Muscular Dystrophy Campaign grant on congenital muscular dystrophy, the MRC Neuromuscular Centre Biobank, Great Ormond Street Hospital Charity and European BIO-NMD FP7 consortium. The National Specialised Commissioning Team (NSCT) funding for the Congenital Muscular Dystrophies and Congenital Myopathy service in London is gratefully acknowledged. Iowa Wellstone Muscular Dystrophy Cooperative Research Center, U54, NS053672, National Institute of Neurological Disorders and Stroke for T.W., S.A.M., K.P.C. and F.M.. K.P. Campbell is an investigator of the Howard Hughes Medical Institute.

Supplementary material

Supplementary material is available at *Brain* online.

Web resources

The Variant Call Format and VCFtools, Petr Danecek, Adam Auton, Goncalo Abecasis, Cornelis A. Albers, Eric Banks, Mark A. DePristo, Robert Handsaker, Gerton Lunter, Gabor Marth, Stephen T. Sherry, Gilean McVean, Richard Durbin and 1000 Genomes Project Analysis Group, Bioinformatics, 2011, http://vcftools.sourceforge.net/; Tennessen JA, Bigham AW, O'Connor TD, Fu W, Kenny EE, Gravel S, McGee S, Do R, Liu X, Jun G, Kang HM, Jordan D, Leal SM, Gabriel S, Rieder MJ, Abecasis G, Altshuler D, Nickerson DA, Boerwinkle E, Sunyaev S, Bustamante CD, Bamshad MJ, Akey JM; Broad GO; Seattle GO; NHLBI Exome Sequencing Project. Evolution and functional impact of rare coding variation from deep sequencing of human exomes. Science. 2012 Jul 6;337(6090):64-9. Epub 2012 May 17. PubMed PMID: 22604720. http://evs.gs.washington.edu/EVS/

References

Baur S, Marles-Wright J, Buckenmaier S, Lewis RJ, Vollmer W. Synthesis of CDP-activated ribitol for teichoic acid precursors in Streptococcus pneumoniae. J Bacteriol 2009; 191: 1200–10.

Beltran-Valero de Bernabe D, Currier S, Steinbrecher A, Celli J, van Beusekom E, van der Zwaag B, et al. Mutations in the O-mannosyltransferase gene POMT1 give rise to the severe neuronal migration disorder Walker-Warburg syndrome. Am J Hum Genet 2002; 71: 1033–43.

Bonnemann CG, Finkel RS. Sarcolemmal proteins and the spectrum of limb-girdle muscular dystrophies. Semin Pediatr Neurol 2002; 9: 81–99.

Bourteel H, Vermersch P, Cuisset JM, Maurage CA, Laforet P, Richard P, et al. Clinical and mutational spectrum of limb-girdle muscular dystrophy type 2I in 11 French patients. Journal of neurology, neurosurgery, and psychiatry 2009; 80: 1405–8.

Breton C, Snajdrova L, Jeanneau C, Koca J, Imberty A. Structures and mechanisms of glycosyltransferases. Glycobiology 2006; 16: 29R–37R.

Brockington M, Blake DJ, Brown SC, Muntoni F. The gene for a novel glycosyltransferase is mutated in congenital muscular dystrophy MDC1C and limb-girdle muscular dystrophy 2I. Neuromuscul Disord 2002; 12: 233–4.

Brockington M, Blake DJ, Prandini P, Brown SC, Torelli S, Benson MA, et al. Mutations in the fukutin-related protein gene (FKRP) cause a form of congenital muscular dystrophy with secondary laminin alpha2 deficiency and abnormal glycosylation of alpha-dystroglycan. Am J Hum Genet 2001a; 69: 1198–209.

Brockington M, Torelli S, Sharp PS, Liu K, Cirak S, Brown SC, et al. Transgenic overexpression of LARGE induces alpha-dystroglycan hyperglycosylation in skeletal and cardiac muscle. PloS One 2010; 5: e14434.

Brockington M, Yuva Y, Prandini P, Brown SC, Torelli S, Benson MA, et al. Mutations in the fukutin-related protein gene (FKRP) identify limb-girdle muscular dystrophy 2I as a milder allelic variant of congenital muscular dystrophy MDC1C. Hum Mol Genet 2001b; 10: 2851–9.

Brown SC, Winder SJ. Dystroglycan and dystroglycanopathies: Report of the 187th ENMC Workshop 11-13 November 2011, Naarden, The Netherlands. Neuromuscul Disord 2012; 22: 659–68.

Cirak S, Herrmann R, Ruthland P, Brockmann K, Korinthenberg R, Nürnberg P, et al. P097 A new locus for an autosomal recessive congenital muscular dystrophy without brain involvement maps to chromosome 7p21. Eur J Paediatr Neurol 2009; 13 (Suppl 1): S51.

Clement E, Mercuri E, Godfrey C, Smith J, Robb S, Kinali M, et al. Brain involvement in muscular dystrophies with defective dystroglycan glycosylation. Ann Neurol 2008; 64: 573–82.

DePristo MA, Banks E, Poplin R, Garimella KV, Maguire JR, Hartl C, et al. A framework for variation discovery and genotyping using next-generation DNA sequencing data. Nat Genet 2011; 43: 491–8.

Devisme L, Bouchet C, Gonzales M, Alanio E, Bazin A, Bessieres B, et al. Cobblestone lissencephaly: neuropathological subtypes and correlations with genes of dystroglycanopathies. Brain 2012; 135 (Pt 2): 469–82.

Dincer P, Balci B, Yuva Y, Talim B, Brockington M, Dincel D, et al. A novel form of recessive limb-girdle muscular dystrophy with mental retardation and abnormal expression of alpha-dystroglycan. Neuromuscul Disord 2003; 13: 771–8.

Dubowitz V, Sewry C. Muscle biopsy: a practical approach. 3rd edn. Oxford: Saunders Elsevier; 2007.

Duclos F, Straub V, Moore SA, Venzke DP, Hrstka RF, Crosbie RH, et al. Progressive muscular dystrophy in alpha-sarcoglycan-deficient mice. J Cell Biol 1998; 142: 1461–71.

Ervasti JM, Campbell KP. Membrane organization of the dystrophin-glycoprotein complex. Cell 1991; 66: 1121–31.

Fukuyama Y, Kawazura M, Haruna H. A peculiar form of congenital progressive muscular dystrophy: report of fifteen cases. Paediat Univ Tokyo 1960; 4: 5–8.

Godfrey C, Clement E, Mein R, Brockington M, Smith J, Talim B, et al. Refining genotype phenotype correlations in muscular dystrophies with defective glycosylation of dystroglycan. Brain:a journal of neurology 2007; 130 (Pt 10): 2725–35.

Godfrey C, Foley AR, Clement E, Muntoni F. Dystroglycanopathies: coming into focus. Current opinion in genetics & development 2011; 21: 278–85.

Hara Y, Balci-Hayta B, Yoshida-Moriguchi T, Kanagawa M, Beltran-Valero de Bernabe D, Gundesli H, et al. A dystroglycan mutation associated with limb-girdle muscular dystrophy. New Engl J Med 2011; 364: 939–46.

Inamori K, Yoshida-Moriguchi T, Hara Y, Anderson ME, Yu L, Campbell KP. Dystroglycan function requires xylosyl- and glucuronyltransferase activities of LARGE. Science 2012; 335: 93–6.

Jimenez-Mallebrera C, Torelli S, Feng L, Kim J, Godfrey C, Clement E, et al. A comparative study of alpha-dystroglycan glycosylation in dystroglycanopathies suggests that the hypoglycosylation of alpha-dystroglycan does not consistently correlate with clinical severity. Brain Pathol 2009; 19: 596–611.

Kanagawa M, Toda T. The genetic and molecular basis of muscular dystrophy: roles of cell-matrix linkage in the pathogenesis. J Hum Genet 2006; 51: 915–26.

Kobayashi K, Nakahori Y, Miyake M, Matsumura K, Kondo-Iida E, Nomura Y, et al. An ancient retrotransposal insertion causes Fukuyama-type congenital muscular dystrophy. Nature 1998; 394: 388–92.

Kunz S, Sevilla N, McGavern DB, Campbell KP, Oldstone MB. Molecular analysis of the interaction of LCMV with its cellular receptor [alpha]-dystroglycan. J Cell Biol 2001; 155: 301–10.

Lefeber DJ, de Brouwer AP, Morava E, Riemersma M, Schuurs-Hoeijmakers JH, Absmanner B, et al. Autosomal recessive dilated cardiomyopathy due to DOLK mutations results from abnormal dystroglycan O-mannosylation. PLoS Genet 2011; 7: e1002427.

Lefeber DJ, Schonberger J, Morava E, Guillard M, Huyben KM, Verrijp K, et al. Deficiency of Dol-P-Man synthase subunit DPM3 bridges the congenital disorders of glycosylation with the dystroglycanopathies. Am J Hum Genet 2009; 85: 76–86.

Li H, Durbin R. Fast and accurate short read alignment with Burrows-Wheeler transform. Bioinformatics 2009; 25: 1754–60.

Li H, Handsaker B, Wysoker A, Fennell T, Ruan J, Homer N, et al. The sequence alignment/map format and SAMtools. Bioinformatics 2009; 25: 2078–9.

Lommel M, Cirak S, Willer T, Hermann R, Uyanik G, van Bokhoven H, et al. Correlation of enzyme activity and clinical phenotype in POMT1-associated dystroglycanopathies. Neurology 2010; 74: 157–64.

Longman C, Brockington M, Torelli S, Jimenez-Mallebrera C, Kennedy C, Khalil N, et al. Mutations in the human LARGE gene cause MDC1D, a novel form of congenital muscular dystrophy with severe mental retardation and abnormal glycosylation of alpha-dystroglycan. Hum Mol Genet 2003; 12: 2853–61.

McDearmon EL, Burwell AL, Combs AC, Renley BA, Sdano MT, Ervasti JM. Differential heparin sensitivity of alpha-dystroglycan binding to laminins expressed in normal and dy/dy mouse skeletal muscle. J Biol Chem 1998; 273: 24139–44.

McDearmon EL, Combs AC, Ervasti JM. Differential Vicia villosa agglutinin reactivity identifies three distinct dystroglycan complexes in skeletal muscle. J Biol Chem 2001; 276: 35078–86.

McDearmon EL, Combs AC, Ervasti JM. Core 1 glycans on alpha-dystroglycan mediate laminin-induced acetylcholine receptor clustering but not laminin binding. J Biol Chem 2003; 278: 44868–73.

McDearmon EL, Combs AC, Sekiguchi K, Fujiwara H, Ervasti JM. Brain alpha-dystroglycan displays unique glycoepitopes and preferential binding to laminin-10/11. FEBS Lett 2006; 580: 3381–5.

McKenna A, Hanna M, Banks E, Sivachenko A, Cibulskis K, Kernytsky A, et al. The Genome Analysis Toolkit: a MapReduce framework for analyzing next-generation DNA sequencing data. Genome Res 2010; 20: 1297–303.

Mercuri E, Brockington M, Straub V, Quijano-Roy S, Yuva Y, Herrmann R, et al. Phenotypic spectrum associated with mutations in the fukutin-related protein gene. Ann Neurol 2003; 53: 537–42.

Mercuri E, Messina S, Bruno C, Mora M, Pegoraro E, Comi GP, et al. Congenital muscular dystrophies with defective glycosylation of dystroglycan: a population study. Neurology 2009; 72: 1802–9.

Messina S, Bruno C, Moroni I, Pegoraro E, D'Amico A, Biancheri R, et al. Congenital muscular dystrophies with cognitive impairment. A population study. Neurology 2010; 75: 898–903.

Michele DE, Barresi R, Kanagawa M, Saito F, Cohn RD, Satz JS, et al. Post-translational disruption of dystroglycan-ligand interactions in congenital muscular dystrophies. Nature 2002; 418: 417–22.

Muntoni F, Voit T. The congenital muscular dystrophies in 2004: a century of exciting progress. Neuromuscul Disord 2004; 14: 635–49.

Murakami T, Hayashi YK, Noguchi S, Ogawa M, Nonaka I, Tanabe Y, et al. Fukutin gene mutations cause dilated cardiomyopathy with minimal muscle weakness. Ann Neurol 2006; 60: 597–602.

Plagnol V, Curtis J, Epstein M, Mok KY, Stebbings E, Grigoriadou S, Wood NW, Hambleton S, Burns SO, Thrasher AJ, Kumararatne D, Doffinger R, Nejentsev S. A robust model for read count data in exome sequencing experiments and implications for copy number variant calling. Bioinformatics 2012; 28: 2747–2754.

Poppe M, Cree L, Bourke J, Eagle M, Anderson LV, Birchall D, et al. The phenotype of limb-girdle muscular dystrophy type 2I. Neurology 2003; 60: 1246–51.

Raitta C, Lamminen M, Santavuori P, Leisti J. Ophthalmological findings in a new syndrome with muscle, eye and brain involvement. Acta ophthalmologica 1978; 56: 465–72.

Roscioli T, Kamsteeg EJ, Buysse K, Maystadt I, van Reeuwijk J, van den Elzen C, et al. Mutations in ISPD cause Walker–Warburg syndrome and defective glycosylation of alpha-dystroglycan. Nat Genet 2012; 44: 581–5.

Stalnaker SH, Aoki K, Lim JM, Porterfield M, Liu M, Satz JS, et al. Glycomic analyses of mouse models of congenital muscular dystrophy. J Biol Chem 2011; 286: 21180–90.

Stalnaker SH, Hashmi S, Lim JM, Aoki K, Porterfield M, Gutierrez-Sanchez G, et al. Site mapping and characterization of O-glycan structures on alpha-dystroglycan isolated from rabbit skeletal muscle. J Biol Chem 2010; 285: 24882–91.

Stalnaker SH, Stuart R, Wells L. Mammalian O-mannosylation: unsolved questions of structure/function. Curr Opin Struct Biol 2011; 21: 603–9.

van Reeuwijk J, Janssen M, van den Elzen C, Beltran-Valero de Bernabe D, Sabatelli P, Merlini L, et al. POMT2 mutations cause alpha-dystroglycan hypoglycosylation and Walker-Warburg syndrome. J Med Genet 2005; 42: 907–12.

Voit T. Congenital muscular dystrophies: 1997 update. Brain Dev 1998; 20: 65–74.

Waite A, Brown SC, Blake DJ. The dystrophin-glycoprotein complex in brain development and disease. Trends Neurosci 2012; 35: 487–96.

Walker AE. Lissencephaly. Arch Neurol Psychiatry 1942; 48: 13–29.

Warburg M. The heterogeneity of microphthalmia in the mentally retarded. Birth defects original article series 1971; 7: 136–54.

Wewer UM, Thornell LE, Loechel F, Zhang X, Durkin ME, Amano S, et al. Extrasynaptic location of laminin beta 2 chain in developing and adult human skeletal muscle. Am J Pathol 1997; 151: 621–31.

Willer T, Lee H, Lommel M, Yoshida-Moriguchi T, de Bernabe DB, Venzke D, et al. ISPD loss-of-function mutations disrupt dystroglycan O-mannosylation and cause Walker-Warburg syndrome. Nat Genet 2012; 44: 575–80.

Yau SC, Bobrow M, Mathew CG, Abbs SJ. Accurate diagnosis of carriers of deletions and duplications in Duchenne/Becker muscular dystrophy by fluorescent dosage analysis. J Med Genet 1996; 33: 550–8.

Yilmaz A, Gdynia HJ, Ponfick M, Ludolph AC, Rosch S, Sechtem U. The proteoglycan-dystrophin complex in genetic cardiomyopathies–lessons from three siblings with limb-girdle muscular dystrophy-2I (LGMD-2I). Clin Res Cardiol 2011; 100: 611–5.

Yoshida A, Kobayashi K, Manya H, Taniguchi K, Kano H, Mizuno M, et al. Muscular dystrophy and neuronal migration disorder caused by mutations in a glycosyltransferase, POMGnT1. Dev Cell 2001; 1: 717–24.